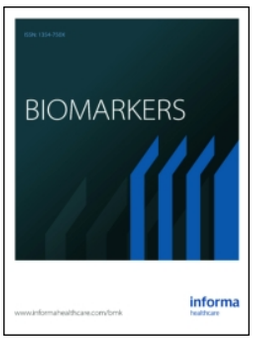

Biomarkers

ISSN: (Print) (Online) Journal homepage: https://www.tandfonline.com/loi/ibmk20

In vitro evaluation of *Annona muricata* L. (Soursop) leaf methanol extracts on inhibition of tumorigenicity and metastasis of breast cancer cells

Aditi Venkatesh Naik & Krishnan Sellappan

To cite this article: Aditi Venkatesh Naik & Krishnan Sellappan (2020): *In vitro* evaluation of *Annona muricata* L. (Soursop) leaf methanol extracts on inhibition of tumorigenicity and metastasis of breast cancer cells, Biomarkers, DOI: 10.1080/1354750X.2020.1836025

To link to this article: https://doi.org/10.1080/1354750X.2020.1836025

BIOMARKERS
https://doi.org/10.1080/1354750X.2020.1836025

Taylor & Francis
Taylor & Francis Group

ORIGINAL ARTICLE

In vitro evaluation of *Annona muricata* L. (Soursop) leaf methanol extracts on inhibition of tumorigenicity and metastasis of breast cancer cells

Aditi Venkatesh Naik[#] and Krishnan Sellappan

Faculty of Life Sciences & Environment, Department of Botany, Goa University, Panjim, India

ABSTRACT

Purpose: The present study evaluates the *in-vitro* anti-tumorigenic potential of leaf methanol extracts of *Annona muricata* (LMAM).

Materials and methods: The cytotoxic activity was assessed in MCF-7 cells by MTT assay at various concentrations ranging from 25–250μg/mL. MCF-7 cells were treated with 50 and 100 μg/mL LMAM for 24 h. To detect LMAM-induced apoptosis; Hoescht 33342 staining along with Cell cycle analysis, Annexin-PI probe as well as oxidative stress damage by reactive oxygen species (ROS) measurements were determined using flow cytometric analysis. While caspase-3 expression levels were studied employing the qRT-PCR method.

Results: LMAM exhibited significant inhibition of MCF-7 cells with an IC_{50} value of 85.55 μg/mL. Hoescht staining showed marked morphological features characteristic of apoptosis in LMAM treated cells. Cell cycle analysis confirmed the proven capability of LMAM showing a 30% rise in G_1 phase upon treatment with 100 μg/mL LMAM, thus inducing cell cycle arrest at G_1 phase and a rise in sub G_0–G_1 population paralleled with a decrease in S phase. Flow cytometric analysis with Annexin V-FITC-PI staining indicated an increase in the early and late apoptotic population with a 3.38% and 19.47% rise respectively when treated with 100 μg/mL LMAM. Treatment with 100 μg/mL LMAM caused an increase in intracellular ROS with MFI value 3334.08. Upregulation of caspase-3 was observed with a 2.18 and 32.47 fold increase compared to control in MCF-7 cells cultured at 50 μg/mL and 100 μg/mL LMAM respectively suggesting caspase-dependent apoptosis.

Conclusion: LMAM proved as a potent ethno-chemopreventive agent and a potential lead in cancer treatment attributable to the synergistic interactive properties of phytoconstituents.

ARTICLE HISTORY
Received 2 August 2020
Accepted 4 October 2020

KEYWORDS
Annona muricata; Acetogenins; Apoptosis; Cancer; MCF-7

1. Introduction

Biomarkers targeted by the advancement of plant-derived therapeutic agents have garnered a lot of attention lately due to their potential in the prevention and treatment of cancer. With the advent of medicine; natural products or phytochemical chemopreventive agents have been used to avert or delay the progression of malignancy and induce optimal changes in the biomarker (Wang *et al.* 2016). Dietary phytochemicals have several built-in benefits over synthetic molecules; owing to its proven efficacy, inexpensivity and oral bioavailability. The separation and identification of a biomarker is an important and tedious matter due to their presence in trace amounts. And this requires the use of highly sensitive and effective methods for monitoring the biomarkers (Ali *et al.* 2011). Besides, there is continued search for more effective biomarkers with the aid of chromatographic techniques to help prevent, inhibit, defer, or cure cancer using bioactive components from natural plants (Za'abi, Ali, *et al.* 2015, Za'abi *et al.* 2016). Therefore, medicinal and aromatic plants continue to attract mankind for medicinal and anthropogenic applications; among them is plant *Annona muricata* widely known for its extensive traditional use and therapeutic benefits.

Annona muricata L. is a flowering plant species within the family Annonaceae; widely found in the world's tropical and subtropical regions, including parts of Africa, America and Asia (Anuragi *et al.* 2016). All organs of this plant are used as ethnomedicine or phytochemical biomarkers to treat diverse diseases and maladies (Moghadamtousi *et al.* 2015a). The plant components have been thoroughly studied till date for their valuable pharmacological properties, embodied by extracts or isolated compounds and were found most effective in the treatment of cancer along with other ailments (Gavamukulya *et al.* 2017, Qazi *et al.* 2018). According to literature, the leaves of *A. muricata* contain 117 isolates of secondary metabolites consisting primarily of alkaloids, phenolic compounds, megastigmanes and annonaceous acetogenins (Matsushige *et al.* 2012, Coria-Téllez *et al.* 2018).

As stated by Morré *et al.* (1994), it has also been shown that the ability of acetogenins to inhibit NADH oxidase is essential for its anti-tumour role via the inhibition of NADH oxidase enzyme function. Besides, acetogenins are also said to obstruct the formation of ATP in mitochondria. This active

CONTACT Krishnan Sellappan skrish@unigoa.ac.in Department of Botany, Goa University, Taleigao Plateau, Panjim 403206, India
[#]Aditi Venkatesh Naik is responsible for statistical design and analysis. E-mail: aditink38@gmail.com (A. V. Naik).

mechanism has shown to be potent towards cancer cells which necessitate higher amounts of ATP requirement compared to normal cells. Thus, this limits the ability of cancer cells to elevate. Besides, the extracts demonstrated stronger toxicity to tumour cells than generic drugs and in certain proportions also improved the viability of healthy cells (Qazi *et al.* 2018).

In plants, leaves account for their highest accumulation of bioactive compounds, which are synthesized as secondary metabolites. Relative to many organic solvents and aqueous media used to retrieve plant-based chemicals, methanol tends to yield better compounds extraction, particularly from the leaves (Kallithraka *et al.* 1995, Fernández *et al.* 2017). The present study was conducted due to extensive scientific literature that gave insight and incentive for further *in vitro* investigations on the biological efficacy of methanol extracts from *A. muricata* (LMAM) to gain an imminent into its production as new agents for agriculture and pharmaceuticals. While major phytochemicals have been identified from *A. muricata*, the potential anti-cancer activity of crude methanolic extracts remains rather obscure. As this notion has not yet been tested, the present study aimed to assess the phytochemical potential and *in-vitro* anti-tumorigenic activity of leaf methanol extracts of *A. muricata* (LMAM) to experimentally justify its role in apoptosis and application in metastasis of breast cancer.

2. Clinical significance

- The present study indicates that leaf methanol extract of *A. muricata* induces apoptosis through the caspase 3 independent pathway involving ROS accumulation and G1 phase arrest with sub G0–G1 population rise and relatable decrease in S phase.
- This was also confirmed by characteristic morphological changes favouring apoptosis. Our research provides empirical evidence for future investigations and calls for the demystification of lead compounds in different organs with substantial anti-cancer sensitivity to cancer type.
- The current findings thus reinforce the scientific evidence for the antitumor potential of this plant used in herbal medicine and its prospects as a potential biomarker for clinical trials in oncology.
- Studies are currently underway to classify organ-specific compounds in *A. muricata* that may be used as therapeutic candidates against cancer. Additionally, studies on the molecular mechanism of A. muricata plant extracts concerning cell protection are currently in progress.

3. Materials and methods

3.1. Preparation of Soursop leaf extract

Fresh and mature leaves of *A. muricata* Linn were procured from KOCL Research Farm, Kirbhatt, Nuvem, South Goa district, Goa, India during the flowering stage (15°18′11.21″N and 73°57′13.29″E). The plant was identified by Dr. S. Krishnan and deposited with a voucher number AVN, AM01516 at Goa University Herbarium, Goa, India. Leaves were cleaned, air-dried for a week, ground to a coarse powder, and then packed into the soxhlet extractor with 95% methanol at 45 °C for 12 h. The filtered extract was concentrated into a molten mass under reduced pressure. Finally, the crude concentrated extract was dried to afford methanol free solid residue. The dried leaf methanolic extract of *A. muricata* (LMAM) was dissolved in 10% w/v DMSO and stored at 0–4 °C until further analysis.

3.2. Cell culture

MCF-7 (breast cancer) cell lines were procured from National Centre for Cell Science (NCCS), Pune and maintained in DMEM medium fortified with 10% v/v Foetal Bovin Serum (FBS) and 1% streptomycin/penicillin in a humidified atmosphere containing 5% CO_2/95% air atmosphere and incubated at 37 °C. When cells achieved ~70% confluence, they were routinely passaged. Confluent cells were washed with 3 mL PBS (Phosphate buffer saline) and trypsinized with 1X trypsin to detach the cells and made into supernatant for seeding. To inhibit the action of trypsin, FBS containing media was added after the detachment of cells. The cell suspension was pelleted at 150× *g* for 5 min, followed by washing with PBS to remove any cell debris. Negative control for all assays was the untreated vehicle-containing DMSO medium (<0.1%).

3.3. In-vitro cytotoxicity assay using MTT

MTT assay was employed to assess the proliferation of cells or cell viability (Mosmann 1983). The cytotoxic potential could be derived from this assay based on the IC_{50} generated. 200 µL of the cells at a concentration of 5×10^3 cells/well were seeded in 96-well plates and maintained for 24 h before treatment. The following day, the cells were treated with a series of 25–250 µg/mL concentrations of LMAM and incubated for 24 h. 20 µL volume of MTT solution [5 mg/mL in phosphate-buffered saline (PBS)] (Sigma, #M2128) was added to each well and then incubated in dark for 3 h at 37 °C. Later, the purple formazan product formed was centrifuged to sediment, and supernatant was discarded cautiously. Finally, 100 µL of DMSO was added to the sediment to solubilize the formazan crystals. The plates were read using ELISA plate reader (Thermo, Multiskan) at an absorbance of 570 nm and 630 nm as reference. The percent viability of MCF-7 cells was expressed as the percent viability of treated cells compared to untreated cells evaluated using the formula:

$$\text{Percentage of viability} = \frac{(\text{Mean Abs. value of untreated cells} - \text{Mean Abs. value of treated cells})}{\text{Mean Abs. of untreated cells}} \times 100$$

The correlation of cell viability and extract concentration was further analyzed using the line regression test and IC_{50} value (extract concentration resulting in 50% cancer cell growth) was determined.

3.4. Hoescht staining for nuclear morphology

The LMAM treated MCF-7 cells were fixed with 4% paraformaldehyde (15 min at 4 °C dark at RT), which were formerly washed with PBS. The cells were then permeabilized with 0.1% Triton-X, incubated at RT for 10 min and washed with cold PBS thrice. Finally, the cells were stained with 500 μL of Hoechst 33342 (1:1000 diluted in 1X PBS) for 10 min (RT in dark) and washed. The stained images were examined under a fluorescence microscope with a 350 nm excitation filter and 460 nm emission filter at 60X magnification (Latt and Wohlleb 1975, Lankadasari *et al.* 2018).

3.5. Cell cycle assay

Using a flow cytometric analysis, changes in the stages of the cell cycle caused by LMAM in MCF-7 cells were analyzed as described by Dobashi *et al.* (2003). Briefly, MCF-7 cells (3×10^5 cells/mL) were seeded in a 6 well-plate and incubated overnight to attach and attain their morphology. The next day, cells were washed with PBS and 1.8 mL of DMEM media was added to each well. Further, cells were treated with 200 μL of LMAM for 24 h (50 μg/mL and 100 μg/mL). After trypsinization, cells were harvested and washed with 1 mL ice-cold PBS. The pellet was resuspended and fixed with ice-cold 70% ethanol and further incubated at 4 °C. After 45 min of incubation time, the cells were again washed with PBS and resuspended in 100 μL of PBS containing RNase A (1 mg/mL) for 30 min at 37 °C. RNase A was used to cleave the RNA and allow PI to intercalate to DNA molecules. Fixed cells were further stained with 5 μL of propidium iodide (1 mg/mL). The mixture solutions were incubated for another 15 min in dark on ice followed by resuspension in 200 μL 1X PBS. The cells were run on BD FACSAria™II system and the resulting DNA distributions were analyzed by Multicycle software available within FCS Express Software (De Novo Software, USA) to determine the proportions of cells in G_0/G_1, S phase, and G_2/M phases of the cell cycle.

3.6. Annexin-V-FITC assay

Distribution of early, late apoptotic or necrotic cells by LMAM was investigated using Annexin-V/PI staining assay (Mohammed *et al.* 2019). MCF-7 cells (3×10^5) were seeded in 6-well plates and incubated overnight following treatment with LMAM (50 μg/mL and 100 μg/mL) and vehicle DMSO for 24 h. Adherent and suspended cells were harvested after the incubation period and washed once with PBS and trypsinized. Cells were re-suspended in 1 mL ice-cold PBS, followed by centrifugation at 350× *g* for 5 min. Pellets were re-suspended in Annexin-V binding buffer (Catalog no. 556547, BD Biosciences, San Jose, CA) and stained with Annexin-V-FITC (BD) and PI (Sigma) according to vendor's instructions. Next, flow cytometry (BD FACSAria™II, San Jose, CA, USA) system was used to analyze the apoptotic and necrotic cell populations in treated and untreated MCF-7 cells. PI was used for necrosis detection, which otherwise cannot penetrate the intact membrane of cells while Annexin-V in combination with PI was used to differentiate cells undergoing apoptosis or necrosis.

3.7. Measurement of intracellular ROS

The level of intracellular ROS was monitored by flow cytometer using 2′,7′- dichlorodihydrofluorescein diacetate ($DCFH_2$-DA) as described in detail by Lankadasari *et al.* (2018). DCFH-DA, a fluorescent stable compound is oxidized by ROS in viable cells. It readily diffuses into cells and in presence of intracellular esterase yields DCHF, which is trapped within cells. DCHF is oxidized to highly fluorescent probe DCF by hydrogen peroxide or low molecular weight peroxides produced by cells. In the current study, MCF-7 cells were treated with LMAM (50 μg/mL and 100 μg/mL) for 24 h. At the end of the treatment, cells were incubated with 10 μL of 1 mM DCFDA (Thermo Fisher Scientific, #D399) working solution at 37 °C for 30 min in dark. Cells were then washed with 1X PBS and the DCF fluorescence intensity measurement was assessed using a flow cytometer (BD FACSAria™II).

3.8. RT-PCR analysis for caspase-3 activity

Apoptotic activity of LMAM treated MCF-7 cells was detected using RT-PCR. In brief, MCF-7 cells were treated with 50 μg/mL and 100 μg/mL of LMAM and incubated for 24 h. Total RNA was extracted from cell lines using TRIzol method. RNA was quantified using nanodrop, following which cDNA was synthesized from 600 ng/mL RNA using a high capacity RNA-to-cDNA kit (Invitrogen). Quantitative real-time PCR was carried out using SYBR Green PCR Master Mix (Invitrogen). The primers used are listed as follows:

- F – 5′-GTGGAATTGATGCGTGATGTTTC-3′
- R – 5′-ATGGCTCAGAAGCACACAAAC-3′

The gene expression level was then calculated as described by Mohammed *et al.* (2019) and the relative expression levels were calculated as ΔΔCt (comparative threshold) $=\Delta Ct$ (Treated) $-$ ΔCt (Control). The calculated expression levels were expressed as an *n*-fold difference relative to the reference gene.

3.9. Flow cytometry data and statistical analysis

The flow cytometry data for cell cycle, apoptosis, and ROS production were analyzed using FCS Express software (DE NOVO Software, Pasadena, CA). The statistical significance of the results was analyzed using GraphPad Prism software version 8.3.1 (San Diego, CA).

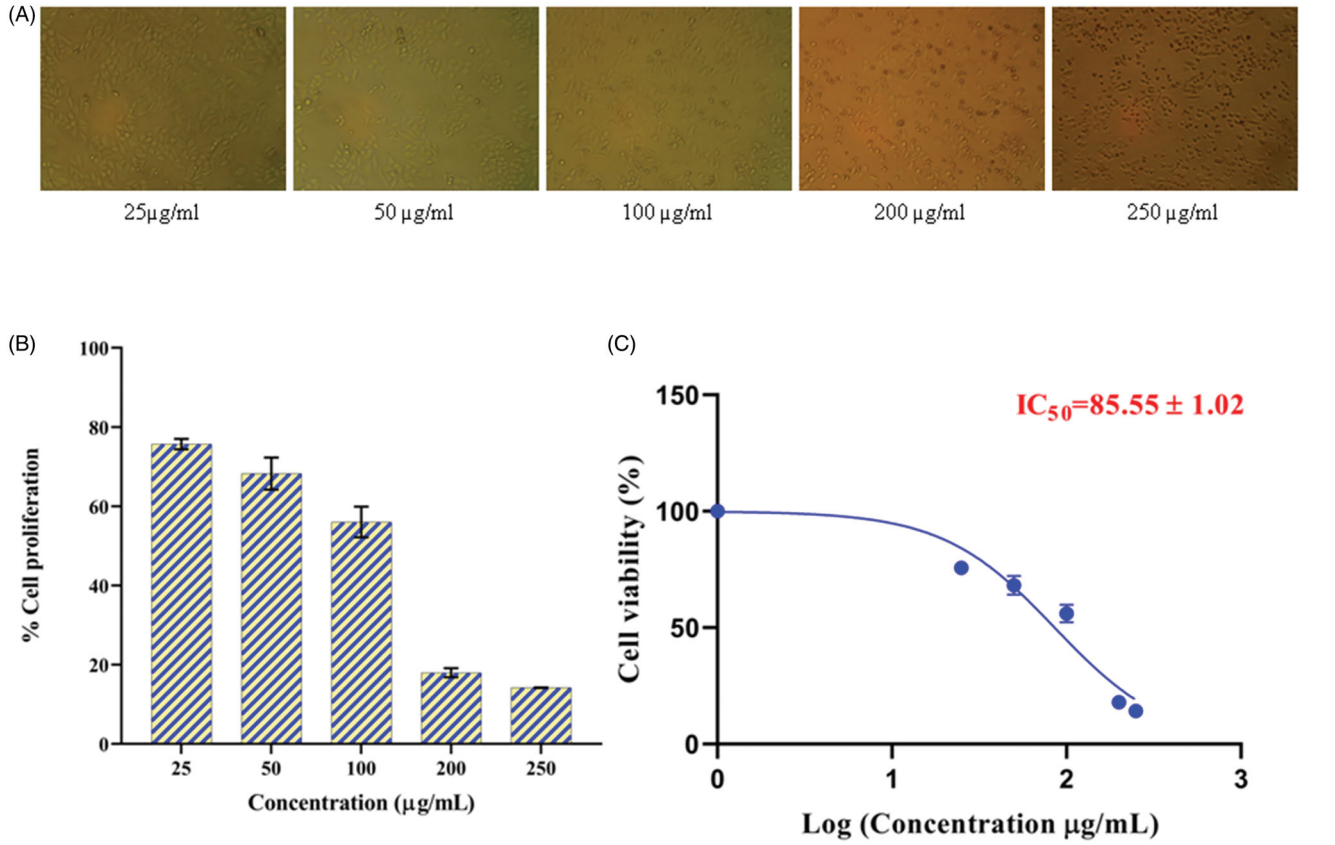

Figure 1. Effect of LMAM on cell viability of MCF-7 cancer cells (A) Representative images showing dose dependent effect of *A. muricata* leaf extract on morphology of breast cancer (MCF-7) cells (magnification X100) (B) Dose-dependence of *A. muricata* L. leaf extract on tumour cell proliferation (C) Data analyzed by non-linear regression, and fitted to linear range of sigmoidal dose-response curves, expressed as log concentration versus normalized percent cell viability. Data points on the graph are mean values, while the solid line represents the linear least square fit of the data..

4. Results

4.1. LMAM suppressed the proliferation of breast cancer cells

The leaf extract of *A. muricata* elicited suppressive effects on breast cancer cells. Figure 1 shows the growth inhibitory effect of LMAM on the proliferation of MCF-7 cells. Upon treatment with LMAM for 24 h, the MCF-7 cell numbers reduced dose-dependently with marked inhibitory effect by the extract. The IC_{50} value towards MCF-7 cells was found to be 85.55 ± 1.02. It should be noted that LMAM did not reveal any noteworthy growth inhibitory potential to non-tumorigenic human breast epithelial cells MCF-10A compared to breast cancer cells. DMSO (0.1%) showed no evidence of toxicity used as vehicle control. The MTT findings suggest the LMAM induced suppressive effect is selective towards breast cancer cells.

4.2. LMAM effect on morphological changes

MCF-7 cells were stained with cell-permeable DNA dye Hoescht 33342 to assess the proportion of cellular damage to explore the nuclear morphological changes in response to LMAM treatment. A typical image of untreated cells exhibited normal form with round intact nuclei (Figure 2). The proliferation was rapid with firm intercellular connections. In contrast, LMAM treated cells displayed typical morphological alterations of apoptosis, including round and altered cell membrane, chromatin condensation, loosened inter-cellular connections, bleb formation in the nucleus, phase bright nuclear fragmentation, and slowed proliferation. Additionally, there was a steady dose-dependent decline in cell numbers in a manner accompanied by reductions in cellular volume and bright condensed staining.

4.3. Cell cycle analysis of LMAM mediated proliferation and apoptosis in MCF-7 cells

To elucidate the mechanism of growth inhibition induced by LMAM and to distinguish between proliferation and apoptosis alterations, we examined the distribution of the cell cycle phases via flow cytometry. As depicted in Figure 3, the substantial dose-dependent arrest of the G_1 phase occurred in the treated breast cancer cells. The G_1 population was increased by 21.10% and 30.48% after 24 h at 50 and 100 µg/mL LMAM treatments respectively. The proportion of cells regarded as apoptotic cells in the DNA histogram in the sub-G_0/G_1 phase with fragmented DNA significantly elevated after 24 h of treatment. This rise in the sub-G_0/G_1 population paralleled a concomitant decrease in S phase promoting cell cycle arrest at the G1 phase.

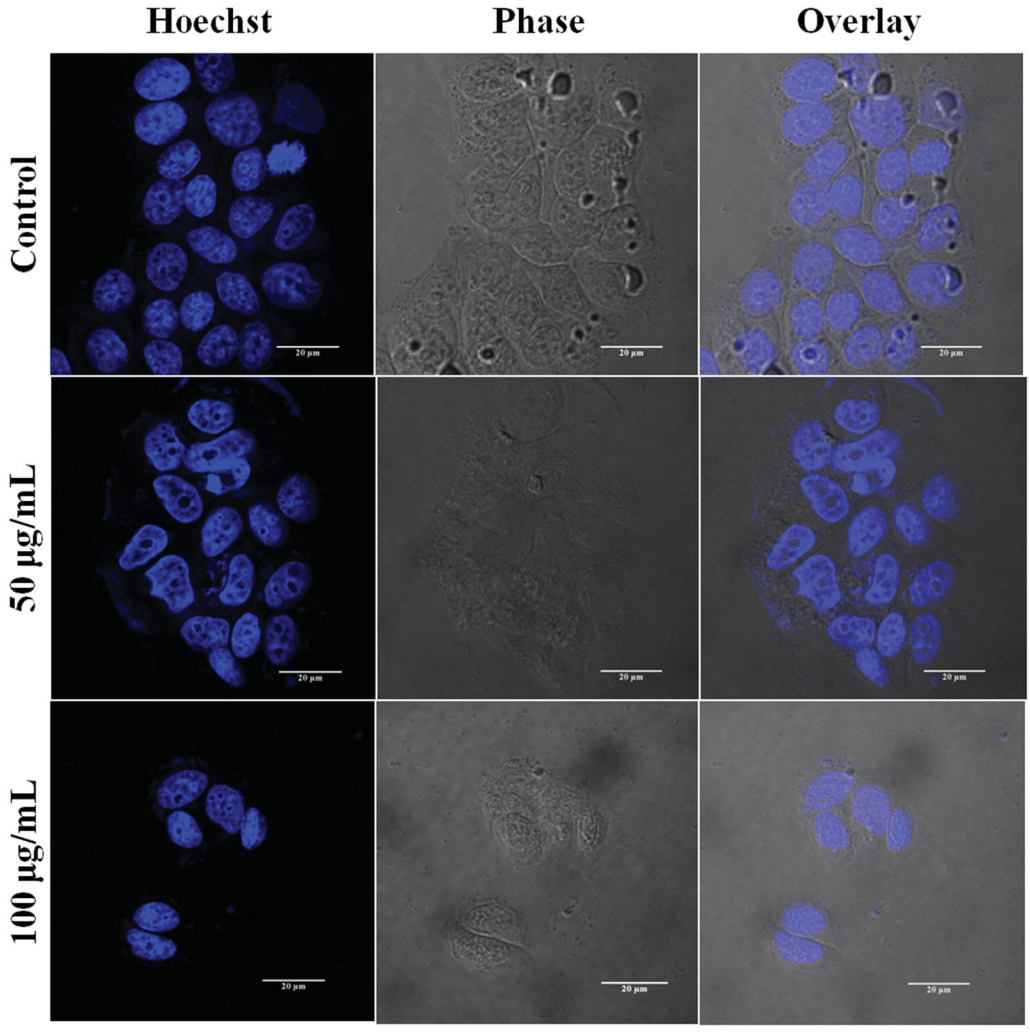

Figure 2. Representative images of breast cancer cells after 24 h treatment with LMAM (50 µg/mL and 100 µg/mL), stained with Hoescht 33342, and observed under fluorescence microscope (magnification 60×). LMAM caused marked elevation in fluorescent intensity which increased in a dose-dependent manner.

4.4. Apoptosis assessment by annexin V-FITC/PI cytometric assay

The apoptotic effect of LMAM was explored by the externalisation of phosphatidylserine (PS) in MCF-7 cells by Annexin-V-FITC and PI double co-staining flow cytometric assay. Cells stained with Annexin-V (AV) and PI probe can be distinguished into four categories. Cell populations occurring in the quadrants of AV+/PI− and AV+/PI+ were defined as early and late apoptotic respectively. While cell populations presented in the lower left (AV−/PI−) of the density plot quadrants was determined as viable cells. *A. muricata* extract decreased the viable population of MCF-7 cells from 83% in untreated cells to 75.49% at 100 µg/mL dose of LMAM (Figure 4). Interestingly, there was an upsurge in the population of dead cells with an apparent increase in the necrotic cell population at 50 µg/mL LMAM which decreased upon treatment at 100 µg/mL LMAM; showing no relevance to dose effect. Such discrepant observations at 50 µg/mL and 100 µg/mL doses may buttress the possibilities of different mechanisms and action sites in metastasis of tumour cells. Furthermore, as the two doses did not show marked responsiveness to LMAM sensitivity does not negate its anticancer potentials. Nevertheless, following treatment with LMAM, both the percentage of early and late apoptotic cells have been dose-dependently enhanced. After 24 h of treatment (100 µg/mL), the early apoptotic percentage of MCF-7 cells was raised to 3.38%, while the late apoptotic population was increased to 19.47% which implies that LMAM can effectively persuade apoptosis in breast cancer cells.

4.5. LMAM stimulates ROS activation

Generation of intracellular ROS has the propensity to trigger various stresses and may lead to metabolic impairments, cell cycle arrest, or cellular apoptosis. ROS production was measured, to evaluate whether LMAM generates oxidative injury in MCF-7 cells. The dose-dependent escalation in ROS amount was produced in treated breast cancer cells relative to untreated cells (Figure 5). ROS formation in untreated cells was found to be at the baseline level. However, simulation of unimodal populations of cells revealed elevated production of cellular ROS with MFI values 1664.74 and 3334.08 upon treatment at 50 µg/mL and 100 µg/mL of LMAM respectively. Observed findings indicate that apoptosis

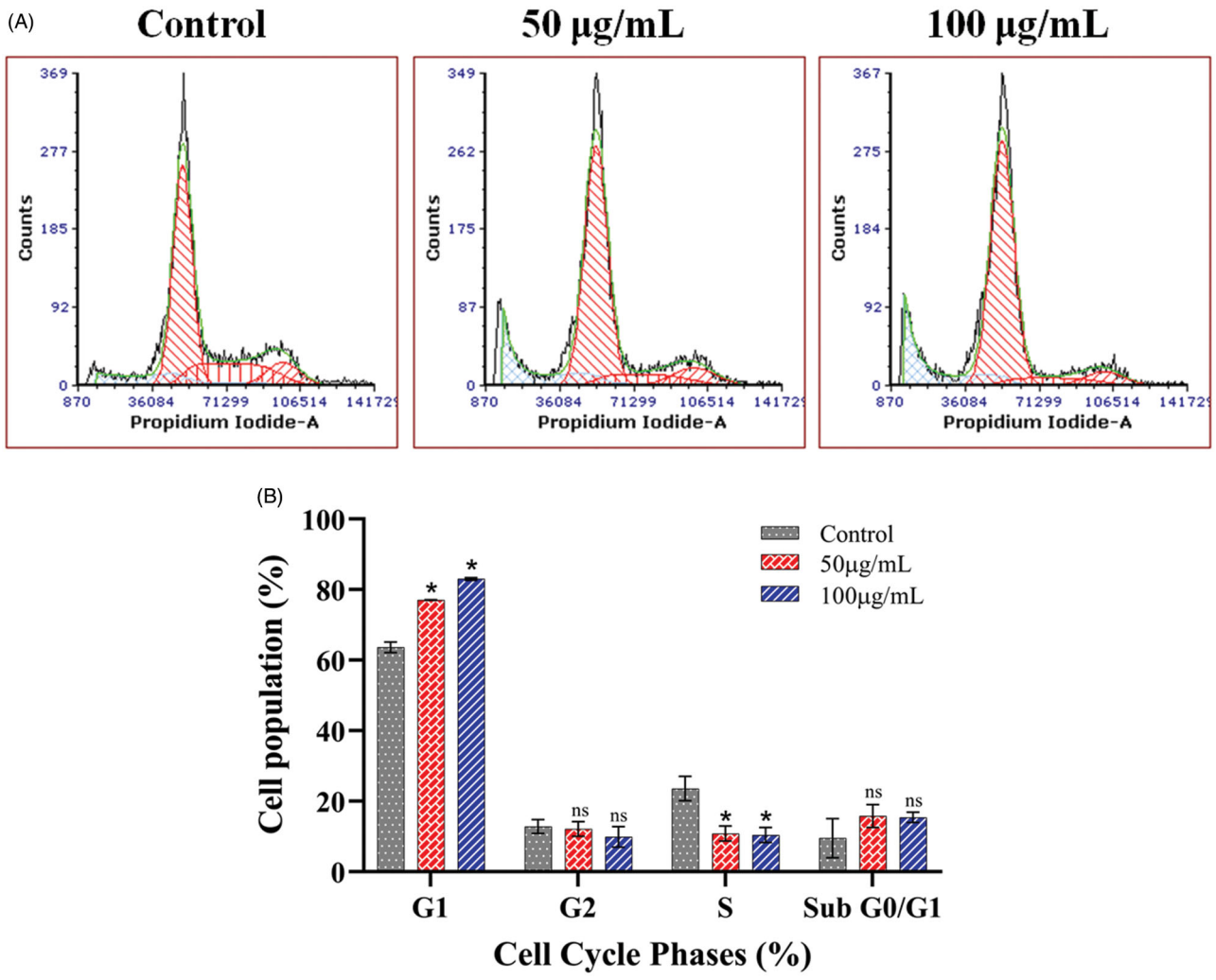

Figure 3. Flow cytometric analysis. (A) Cell cycle arrest of breast cancer cells treated with LMAM in a dose-dependent manner. (B) The representative bar charts depict significant cell cycle arrest at G1 phase after 24 h treatment. The data represent the means ± SD of three independent experiments. $^{*}p < 0.0001$ compared with the untreated control group.

activation by LMAM is likely to be facilitated by increased production of ROS contributing to an oxidative stress-dependent approach of apoptosis in MCF-7 cells.

4.6. LMAM triggered caspase-3 activation

The energy-dependent apoptosis cycle heavily depends on the caspase family, or cysteinyl aspartate proteinase, to spatially transform the triggering cellular stimuli into ultimate cell death. Caspase-3 is deemed the most critical of executioner caspases, leading to morphological changes, notably cell contraction, chromatin condensation, development of apoptotic bodies accompanied by apoptotic cell phagocytosis. In MCF-7 cells, the degree of apoptosis was determined by measuring the level of caspase-3 activation following LMAM exposure (Figure 6). LMAM treatment activated the caspase-3 activity in a dose-dependent manner. A pronounced up-regulation was observed with a 32.47 fold increase ($p < 0.005$) in caspase-3 of mRNA levels in MCF-7 cells cultured at 100 µg/mL, while 50 µg/mL LMAM showed 2.18-fold increase compared to control, suggesting that LMAM induced apoptosis involving caspase-3 activation.

5. Discussion

Medicinal plants are invaluable resources for treating varied ailments and highly valued by patients as a substitute and complementary cancer-fighting medicine (Schmidt *et al.* 2007). Identification of potential plant-derived cancer cell-specific biomarkers has prompted many investigators in their attempts to find active apoptotic-inducing agents to lessen the tumour burden (Newman and Cragg 2016). Extracts of *A. muricata* can impede proliferation and induce apoptosis in *in-vitro* cancer cells including *in-vivo* mice models and inhibit tumour metastasis providing an option for cancer ethnomedicinal treatment (Fernández *et al.* 2017).

The activity of *A. muricata* is considered attributable to the biosynthesis of secondary metabolites such as alkaloids, phenols, flavonoids, and most peculiar group of compounds notably annonaceous acetogenins in different plant parts (Chan *et al.* 2020). However, this plant obtained from different cultivations may not have the same palliative effects on cancer (Syed Najmuddin *et al.* 2017, Yajid *et al.* 2018). Thus, we first investigated various plant organs in our preliminary work namely rind, pulp, seed, leaf, bark, and roots in terms

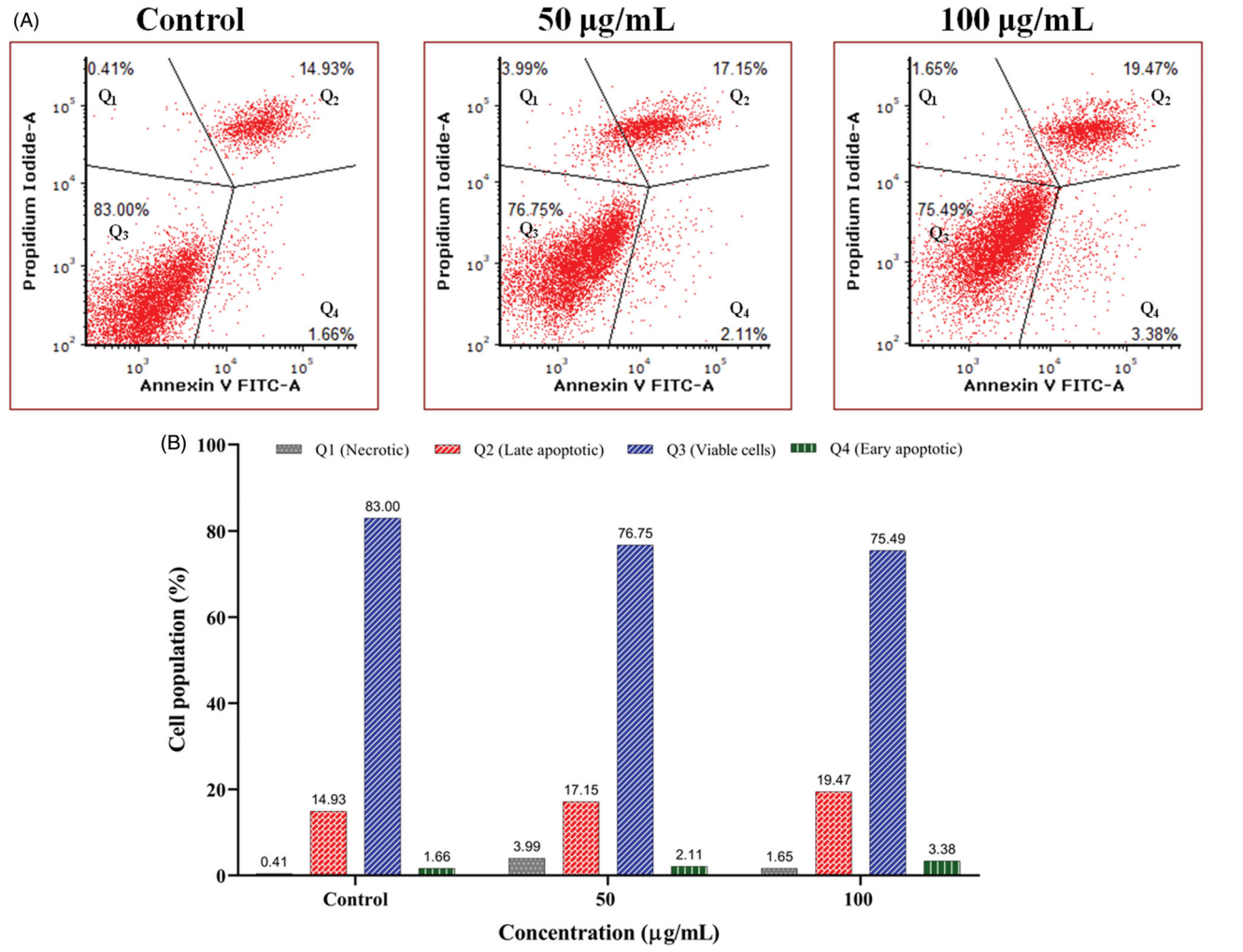

Figure 4. Annexin V-FITC and PI staining indicates (A) dose dependent apoptosis rates of breast cancer cells treated with LMAM detected by flow cytometry after 24 h. (B) The bar charts illustrate the percentage of MCF-7 cells undergoing early and late apoptosis.

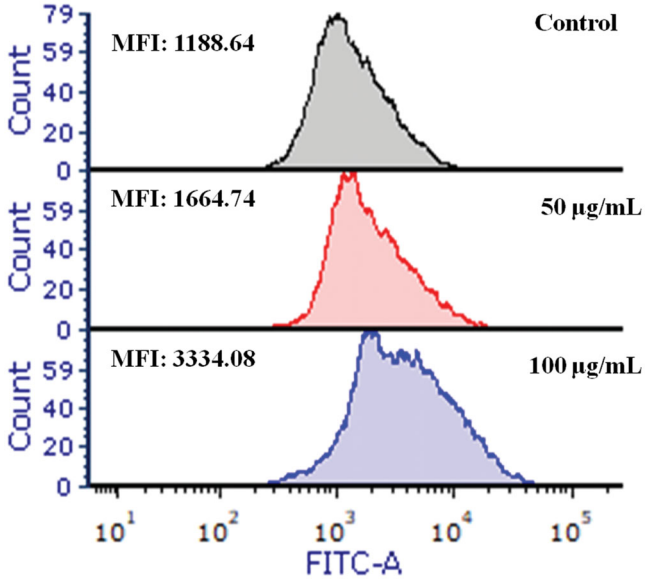

Figure 5. Variation of ROS production in breast cancer cells treated with LMAM. LMAM triggered the production of ROS dose dependently monitored by flow cytometry, where MFI represents median of fluorescence.

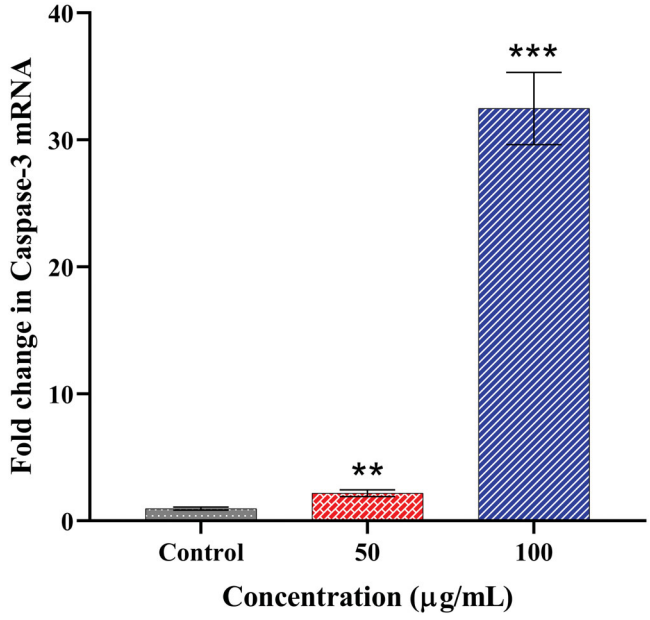

Figure 6. Quantitative real time RT-PCR (qRT-PCR) of caspase-3 gene in LMAM treated MCF-7 breast cancer cell lines. The expression of mRNA is given by means of fold increase. Data represents the means ± SD of three independent experiments. $^{*}p < 0.0001$ compared with the untreated control group. $^{**}p < 0.005$; $^{***}p < 0.005$ versus control.

of extraction yields (Naik and Sellappan 2019, 2020) and comparative anti-proliferative activities. While several researchers reported the fruit displaying potent anti-cancer activity, our study showed that the leaf extract derived from methanol solvent extraction possessed comparatively better anti-oxidant and anti-proliferative capacity while also serving better raw materials as they are more profuse and accessible (Jaramillo *et al.* 2000, Renu *et al.* 2017, Wahab *et al.* 2018, Murthy and Bapat 2019, Roduan *et al.* 2019).

In this study, we investigated the apoptosis-inducing and/or cell cycle arresting efficacy of *A. muricata* leaf methanol extracts to reveal the possible mechanism for regulating or inhibiting the growth of MCF-7 breast cancer cells stimulated by LMAM. Our study implies that LMAM could induce inhibitory effects in a dose-dependent manner in MCF-7 cancer cells without inflicting cytotoxicity in the normal breast cancer cells, suggesting that LMAM may selectively target specific mechanisms in certain cancer cells as reported in the literature (Coria-Téllez *et al.* 2018, Qazi *et al.* 2018, Yajid *et al.* 2018, Vora *et al.* 2020).

Apoptosis is a vital phase of programmed cell death involving complex phenotypic and biochemical modifications which are crucial hallmarks of apoptosis (Galluzzi *et al.* 2018). In response to LMAM treatment, Hoescht 33342 staining revealed chromatin condensation, DNA fragmentation, and drop in cell numbers in contrast to control cells that exhibited normal cellular architecture without major changes indicative that *A. muricata* extracts caused morphological changes in favour of apoptosis in MCF-7 cells (Pieme *et al.* 2014).

The repression of the cell cycle is closely linked with apoptosis, and cell cycle dysfunction can ultimately lead to apoptotic death. Inhibiting the progression of the deregulated cell cycle in cancer cells is thus another effective strategy for regulating tumour progression. Chemotherapeutic compounds often promote cell cycle interruption during phase G_0/G_1 or phase G_2/M which can effectively enhance its anti-cancer potential (Pieme *et al.* 2014, Moghadamtousi *et al.* 2015b, Liu *et al.* 2016).

To determine whether the arrest of the cell cycle is regulated by LMAM induced growth suppression; we studied the distribution of breast cancer cells across the cell cycle. The S-phase and the G_2/M-phase cells were identified as proliferative states, and the apoptotic phase was identified as sub-G_1-phase. Our data showed that LMAM arrests cell cycle at G_1 phase, which was accompanied by a modest increase in sub-G_0/G_1 phase and a significant decrease in S-phase cells, suggesting that LMAM treatment produced a blockage effect in G_1/S transition attributable to apoptosis activation and sub-G_0/G_1 cell cycle arrest. However, the specific mechanism of LMAM treatment on the machinery of the cell cycle and the expression of several associated proteins warranted further investigations (Moghadamtousi *et al.* 2014, Haykal *et al.* 2019).

Taking another look at the findings obtained from Annexin V-PI staining using MCF-7 cells showed a rise in early and late apoptotic cells when treated dose-dependently with LMAM. Also, we observed bi-phasic effects having minimal relation to the dose-effect where a lower concentration (50 μg/mL) of LMAM caused an uptick in the necrotic cell population followed by a decrease at 100 μg/mL concentration. This bi-phasic response is a frequent occurrence in many anti-cancer agents and well reported by Agu *et al.* (2018) using ethyl acetate extracts of *A. muricata* and an isolated acetogenin namely 15-acetyl guanacone. This finding re-emphasizes the need for further investigations to identify the action mechanism that lies beyond the cell-cycle (Cappelletti *et al.* 2000). This may also be understood on the basis that, in the absence of the intended repair, MCF-7 cells were initially taken into quiescence (G_0/G_1) phase for potential repair of the defect, but were subsequently marked out for cells at the apoptotic level, leading in the shift of cells from the G_0/G_1 level to the apoptotic stage.

The present study showed that concentration-dependent treatment with LMAM significantly increased ROS output in breast cancer cells. The excessive accumulation of ROS caused oxidative damage, among the various initiating triggers for the induction of apoptosis by natural products (Yang *et al.* 2016). These findings indicated that disruption of the mitochondrial membrane could have induced excessive accumulation of ROS in cancer cells as also reported by Moghadamtousi *et al.* (2014).

Intensive molecular studies to date have shown that there are two key apoptotic pathways, namely extrinsic through a death receptor and intrinsic caspase triggered mitochondrial-mediated pathways. The intrinsic cytochrome c pathway stimulates the caspase-9 while the extrinsic route stimulates the caspase-8. Unless these initiator caspases are activated, the apoptosis execution process is triggered via caspase-7,-6 and-3 activation. Expression of caspase protease is the premise of cell apoptosis, and further activation of caspase-3 in the apoptotic mechanism is a crucial downstream effect (Moghadamtousi *et al.* 2014, 2015b). Our results showed that treatment with LMAM elevated caspase-3 activities. It is thus postulated that apoptosis activation is through a mitochondrial-mediated cascade in the breast cancer cells notably closely related to the occurrence of bioactive components in *A. muricata* extracts namely potent alkaloids, phenols, flavonoids, and acetogenins (ACG) (Pieme *et al.* 2014, George *et al.* 2015, Abdullah *et al.* 2017, Syed Najmuddin *et al.* 2017).

Over 100 ACG's have been extracted from *A. muricata*. Several ACG's are reported to possess the toxic potential to varied cancer types. Various sources of evidence suggest that extracts of *A. muricata* repressed the *in-vivo* development of tumours in animals and also caused *in-vitro* toxicity in cancer cell lines. For example, annohexocin, annopentocin A/B/C, annomuricin E, annomutacin, muricoreacin, and muricohexocin A/B/C are toxic to breast MCF-7, prostate PC-3, lung A549, renal A498, pancreatic PACA, and colorectal HT-29 cells (Gavamukulya *et al.* 2017, Coria-Téllez *et al.* 2018, Qazi *et al.* 2018). Similarly, some studies have documented undesirable toxic side effects such as neurodegeneration indicative that ACG's alone may not serve good drug candidates unless chemical modifications can retain apoptotic function and minimize neurotoxicity (Champy *et al.* 2005, Kojima *et al.* 2015). The anti-carcinogenic mechanism and effect can vary

from that of a single defined chemical compound, because active constituents in extracts may exhibit combinational effects. Isolating the lone active compound from extracts cannot only jeopardize therapeutic effectiveness but may render toxic syndrome (Yang *et al.* 2015, 2016, Liu *et al.* 2016).

Yang *et al.* (2015) emphasized the significance of plant-derived whole-composition extracts and compared the anti-cancer potential of enriched acetogenin and flavonoid fractions from *A. muricata* along with pure chemical compounds. It was reported that phytochemical synergy in whole extracts was more effective in suppressing proliferation compared to isolated fractions or pure compounds in prostate cancer cells. It also indicates that whole extract may be superior over chemically isolated single compounds and deserves further study for therapeutic use. In our study, we also further confirmed the anti-tumour activity of LMAM *in-vivo* and found that LMAM significantly inhibited tumour growth in swiss albino mice and improved the life span of treated mice without major changes in toxicity parameters evaluated.

6. Conclusion

In conclusion, our study showed that the leaf methanol extracts of *A. muricata* inhibited the proliferation of breast cancer cells, leading to cell cycle arrest and programmed cell death through the involvement of ROS and upregulation of caspase-3 signalling pathway. These data suggest that LMAM potentially offers better bioactive compounds with substantial anti-proliferative properties that can be established as a better dietary mechanism-based agent useful in primary health care for cancer prevention and metastasis.

Acknowledgements

The authors are deeply grateful to Dr. Hemant Agrawal, Flowcytometry Solutions for valuable guidance and kind suggestions. The authors also thank Dr. Harikumar K. B, Scientist E-I., Rajiv Gandhi Centre for Biotechnology, Thiruvananthapuram, Kerala for providing facilities and assistance. The authors also wish to thank the International Society for Advancement of Cytometry (ISAC) and Dr. Shyamalina Biswas for kind help and motivation.

Disclosure statement

No potential conflict of interest was reported by the author(s).

Funding

The present work was financially supported by the Department of Science and Technology, New-Delhi in the form of the DST INSPIRE Fellowship [IF160005] and by the Council for Scientific and Industrial Research, New-Delhi, India [38(1471)/18/EMR-II].

ORCID

Aditi Venkatesh Naik http://orcid.org/0000-0002-1675-665X
Krishnan Sellappan http://orcid.org/0000-0001-7367-9542

References

Abdullah, M., *et al.* 2017. The value of caspase-3 after the application of *Annona muricata* leaf extract in COLO-205 colorectal cancer cell line. *Gastroenterology research and practice*, 2017, 4357165.

Agu, K.C., *et al.* 2018. *In vitro* anticancer assessments of *Annona muricata* fractions and in vitro antioxidant profile of fractions and isolated acetogenin (15-acetyl guanacone). *Journal of cancer research and practice*, 5 (2), 53–66.

Ali, I., *et al.* 2011. Role of chromatography for monitoring of breast cancer biomarkers. *Recent pat biomark*, 1 (1), 89–97.

Anuragi, H., *et al.* 2016. Molecular diversity of *Annona* species and proximate fruit composition of selected genotypes. *3 biotech*, 6 (2), 204.

Cappelletti, V., *et al.* 2000. Genistein blocks breast cancer cells in the G2M phase of the cell cycle. *Journal of cellular biochemistry*, 79 (4), 594–600.

Champy, P., *et al.* 2005. Quantification of acetogenins in *Annona muricata* linked to atypical Parkinsonism in Guadeloupe. *Movement disorders: official journal of the movement disorder society*, 20 (12), 1629–1633.

Chan, W.J.J., *et al.* 2020. The safety and tolerability of *Annona muricata* leaf extract: a systematic review. *The journal of pharmacy and pharmacology*, 72 (1), 1–16.

Coria-Téllez, A.V., *et al.* 2018. *Annona muricata*: a comprehensive review on its traditional medicinal uses, phytochemicals, pharmacological activities, mechanisms of action and toxicity. *Arabian journal of chemistry*, 11 (5), 662–691.

Dobashi, Y., Takehana, T., and Ooi, A., 2003. Perspectives on cancer therapy: cell cycle blockers and perturbators. *Current medicinal chemistry*, 10 (23), 2549–2558.

Fernández, A.E.L., *et al.* 2017. Evaluation of emerging methods on the polyphenol content, antioxidant capacity and qualitative presence of acetogenins in Soursop pulp (*Annona muricata* L.). *Revista Brasileira de Fruticultura*, 39, 1–8.

Galluzzi, L., *et al.* 2018. Molecular mechanisms of cell death: recommendations of the Nomenclature Committee on Cell Death 2018. *Cell death and differentiation*, 25 (3), 486–541.

Gavamukulya, Y., Wamunyokoli, F., and El-Shemy, H.A., 2017. *Annona muricata*: is the natural therapy to most disease conditions including cancer growing in our backyard? A systematic review of its research history and future prospects. *Asian pacific journal of tropical medicine*, 10 (9), 835–848.

George, V.C., *et al.* 2015. Antioxidant, DNA protective efficacy and HPLC analysis of *Annona muricata* (soursop) extracts. *Journal of food science and technology*, 52 (4), 2328–2335.

Haykal, T., *et al.* 2019. *Annona cherimola* seed extracts activates extrinsic and intrinsic apoptosis pathways in leukemia cells. *Toxins*, 11 (9), 506.

Jaramillo, M.C., *et al.* 2000. Cytotoxicity and antileishmanial activity of *Annona muricata* pericarp. *Fitoterapia*, 71 (2), 183–186.

Kallithraka, S., *et al.* 1995. Survey of solvents for the extraction of grape seed phenolics. *Phytochemical analysis*, 6 (5), 265–267.

Kojima, N., *et al.* 2015. Synthesiz of dansyl-labeled probe of thiophene analogue of annonaceous acetogenins for visualization of cell distribution and growth inhibitory activity toward human cancer cell lines. *Bioorganic & medicinal chemistry*, 23 (6), 1276–1283.

Lankadasari, M.B., *et al.* 2018. Targeting S1PR1/STAT3 loop abrogates desmoplasia and chemosensitizes pancreatic cancer to gemcitabine. *Theranostics*, 8 (14), 3824–3840.

Latt, S.A. and Wohlleb, J.C., 1975. Optical studies of the interaction of 33258 Hoechst with DNA, chromatin, and metaphase chromosomes. *Chromosoma*, 52 (4), 297–316.

Liu, N., *et al.* 2016. Functional proteomic analysis revels that the ethanol extract of *Annona muricata* L. induces liver cancer cell apoptosis through endoplasmic reticulum stress pathway. *Journal of ethnopharmacology*, 189, 210–217.

Matsushige, A., *et al.* 2012. Three new megastigmanes from the leaves of *Annona muricata*. *Journal of natural medicines*, 66 (2), 284–291.

Moghadamtousi, S.Z., *et al.* 2014. *Annona muricata* leaves induce G1 cell cycle arrest and apoptosis through mitochondria-mediated pathway

in human HCT-116 and HT-29 colon cancer cells. *Journal of ethnopharmacology* , 156, 277–289.

Moghadamtousi, S.Z., *et al.* 2015a. *Annona muricata* (Annonaceae): a review of its traditional uses, isolated acetogenins and biological activities. *International journal of molecular sciences*, 16 (7), 15625–15658.

Moghadamtousi, S.Z., *et al.* 2015b. The chemopotential effect of *Annona muricata* leaves against azoxymethane-induced colonic aberrant crypt foci in rats and the apoptotic effect of acetogenin annomuricin E in HT-29 cells: a bioassay-guided approach. *PloS one*, 10 (4), e0122288.

Mohammed, S., *et al.* 2019. Examination of the role of sphingosine kinase 2 in a murine model of systemic lupus erythematosus. *FASEB journal: official publication of the Federation of American Societies for Experimental Biology*, 33 (6), 7061–7071.

Morré, D.J., *et al.* 1994. Mode of action of bullatacin, a potent antitumor acetogenin: inhibiton of NADH oxidase activity of HcLa and HL-60, but not liver, plasma membranes. *Life sciences*, 56 (5), 343–348.

Mosmann, T., 1983. Rapid colorimetric assay for cellular growth and survival: application to proliferation and cytotoxicity assays. *Journal of immunological methods*, 65 (1–2), 55–63.

Murthy H.N. and Bapat V.A. (Eds.), 2019. *Bioactive compounds in underutilized fruits and nuts*. New York, NY: Springer International Publishing, 1–15.

Naik, A.V. and Sellappan, K., 2019. Physicochemical and phytochemical analysis of different plant parts of *Annona muricata* L. (Annonaceae). *Pharmaceutical methods*, 10 (2), 70–78.

Naik, A.V. and Sellappan, K., 2020. Chromatographic fingerprint of essential oils in plant organs of *Annona muricata* L. (Annonaceae) using HPTLC. *Analytical chemistry letters*, 10 (2), 214–226.

Newman, D.J. and Cragg, G.M., 2016. Natural products as sources of new drugs from 1981 to 2014. *Journal of natural products*, 79 (3), 629–661.

Pieme, C.A., *et al.* 2014. Antiproliferative activity and induction of apoptosis by *Annona muricata* (Annonaceae) extract on human cancer cells. *BMC complementary and alternative medicine*, 14 (1), 516.

Qazi, A.K., *et al.* 2018. Emerging therapeutic potential of Graviola and its constituents in cancers. *Carcinogenesis*, 39 (4), 522–533.

Renu, G., Chittibabu, C.V., and Ranjithkumar, A., 2017. A comparative study on the *in-vitro* antioxidant potentials of the stem bark, root, leaf and fruit pulp of *Annona muricata* L. *World journal of pharmaceutical research*, 6 (16), 1029–1043.

Roduan, M.R.M., *et al.* 2019. Cytotoxicity, antitumor-promoting and antioxidant activities of *Annona muricata in vitro*. *Journal of herbal medicine*, 15, 100219.

Schmidt, B.M., *et al.* 2007. Revisiting the ancient concept of botanical therapeutics. *Nature chemical biology*, 3 (7), 360–366.

Syed Najmuddin, S.U.F., *et al.* 2017. Comparative study of antioxidant level and activity from leaf extracts of *Annona muricata* Linn obtained from different locations. *Pertanika journal of tropical agricultural science*, 40 (1), 119–130.

Vora, A.P., *et al.* 2020. *Annona muricata* non-selectively suppress PC3 cells by inhibitng cell proliferation and inducing cell cyclearrest. *The FASEB journal*, 34 (S1), 1.

Wahab, A., *et al.* 2018. Exploring the leaves of *Annona muricata* L. as a source of potential anti-inflammatory and anticancer agents. *Frontiers in pharmacology*, 9, 661.

Wang, N., *et al.* 2016. Discovery of biomarkers for oxidative stress based on cellular metabolomics. *Biomarkers: biochemical indicators of exposure, response, and susceptibility to chemicals*, 21 (5), 449–457.

Yajid, A.I., *et al.* 2018. Potential benefits of *Annona muricata* in combating cancer: a review. *The Malaysian journal of medical sciences*, 25 (1), 5–15.

Yang, C., *et al.* 2015. Synergistic interactions among flavonoids and acetogenins in Graviola (*Annona muricata*) leaves confer protection against prostate cancer. *Carcinogenesis*, 36 (6), 656–665.

Yang, H., Liu, N., and Lee, S., 2016. Ethanol extract of *Annona muricata*. L induces liver cancer cell apoptosis through ROS pathway. *Biomedical and pharmacology journal*, 9 (3), 919–925.

Za'abi, M.A., Ali, B.H., and Ali, I., 2015. Advances in the methodologies for the analysis of acute kidney injury biomarkers. *Recent patents on biomarkers*, 5 (2), 81–92.

Za'abi, M.A., *et al.* 2016. Analyses of acute kidney injury biomarkers by ultra-high performance liquid chromatography with mass spectrometry. *Journal of separation science*, 39 (1), 69–82.